Local Identification of Voltage Emergency Situations

C. D. Vournas, *Fellow, IEEE* T. Van Cutsem, *Fellow, IEEE*

***Abstract*—This paper proposes a simple procedure to identify the onset of long-term voltage instability from the time evolution of the distribution voltages controlled by load tap changers. The moving average of sampled measurements is computed and used to trigger local emergency signals. The method is validated on voltage signals obtained from time simulation of a realistic test system. The ability to identify instability in the critical area is demonstrated in three test cases.**

***Index Terms*—Long-term Voltage Stability, Voltage Collapse, load tap changer, overexcitation limiter, emergency detection.**

I. Introduction

THE two lines of defense against instability and blackout are the assessment and maintenance of adequate security margins against credible events, on one hand, and System Protection Schemes (SPS) against more severe events, on the other hand. Under the pressure of electricity market, it is likely that future power system operation will rely more extensively on the second line of defense. This applies in particular to long-term voltage instability [1, 2], which is of concern in this paper.

Any SPS against voltage instability requires a good identification of the instability onset, in order to apply emergency controls, some of which have considerable economical and social cost, as is the case with load shedding.

It is well known that voltage level by itself is not adequate to provide a reliable, preventive picture of system security margins. However, it is often a good indicator of a post-disturbance emergency situation. Thus, several load-shedding schemes relying on voltage measurements collected near load centers have been demonstrated in the literature (e.g. [3-5]).

In some cases, however, relying solely on voltage for emergency actions may not be satisfactory. For instance:

- when the load response is dominated by induction motors, voltages may drop abruptly when OverExcitation Limiters (OELs) come into play, leaving little time for SPS to act; the same is true when a generator operating at its overexcitation limit is prone to loss of synchronism;
- in some systems, it may be difficult to select a unique voltage threshold, high enough for prompt reaction but low enough to avoid reacting to harmless disturbances [5].

This and other considerations have prompted interest into the detection of impending voltage instability from other real-time measurements. More precisely, schemes are sought to detect a condition that corresponds to the system becoming unstable, rather than observe the consequences of this instability.

In this respect, the availability of affordable Phasor Measurement Units opens exciting perspectives [6]. In some future, the latter might allow to perform state estimation at a high rate, whose output could be used to perform in real-time small-disturbance analyses that are currently limited to off-line simulation studies [7, 8].

The fact remains, however, that SPS design will always favor the use of local measurements, if the latter can be properly processed. This is a matter of simplicity and hence, reliability.

Concerning long-term voltage stability in particular, this prompted interest for voltage instability predictors aimed at detecting at several buses a condition, in which the magnitude of the load impedance becomes equal to that of the Thévenin equivalent impedance seen from the bus of concern (impedance matching condition) [9, 10, 11]. This approach, however, is not free from difficulties. For instance, over the (sampled) measurement time window, the operating conditions should change (for accuracy of estimation), but not to the extent that the assumption of a constant Thévenin impedance would become invalid. Furthermore, when the latter changes under the effect of OEL activations, it takes some time to reach a new estimate from which decision can be taken. These issues need to be addressed in order for the predictor to be applied over the time interval that follows a severe disturbance. Many references so far have concentrated on smooth load increase scenarios, which can be easily monitored through state-of-the-art load power margin computations.

This paper proposes an alternative that is free from the above identification problems and applies to large-disturbance scenarios. Attention is paid to the behaviour of Load Tap Changers (LTCs). It is known for a long time that LTCs can become unstable [12]. They are also a driving force of long-term voltage instability, since by restoring distribution voltages after a disturbance they indirectly restore loads, thus increasing transmission voltage drops and drawing on reactive reserves. When load demand exceeds the capability of the system, a voltage instability situation results [2].

This is reflected in the distribution voltages, as illustrated in Fig. 1, obtained from simulation of a voltage unstable case.

Costas D. Vournas is with the School of Electrical and Computer Engineering at the National Technical University of Athens (NTUA), Iroon Polytechneiou 9, Zographou, Athens, Greece (email: vournas@power.ece.ntua.gr).

Thierry Van Cutsem is with FNRS (Fund for Scientific Research) at the Department of Electrical Engineering and Computer Science (Montefiore Institute) of the University of Liège, Belgium (email: t.vancutsem@ulg.ac.be).

This plot shows the unsuccessful attempt to bring the distribution voltage back inside the deadband (lower limit shown with dotted line), in particular under the effect of an OEL acting near t= 82 s. A simple method is proposed in the paper to detect this situation.

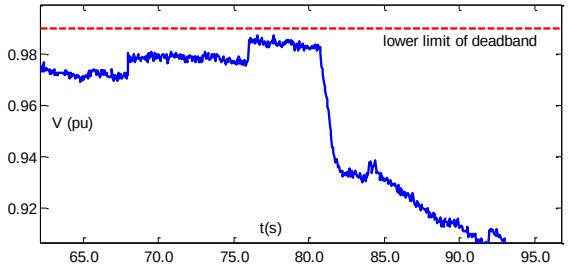

Figure 1: Typical simulated evolution of an LTC-controlled (distribution) voltage in a long-term unstable scenario

The authors are aware of at least one manufacturer that has introduced protection schemes in the LTC logic, in case unsuccessful tap changing is detected [13]. Even though the emergency detection algorithm proposed in this paper is different, this demonstrates the feasibility and applicability of the LTC based approach.

After a brief review in Section II of the instability caused by LTCs, the proposed procedure is described in Section III. Simulations of a small but realistic system are reported in Section IV, while a concluding discussion is offered in Section V.

II. Voltage Instability Mechanism and LTC

A. Modelling and Stability of multi-LTC Systems

We consider in this section a power system whose long-term dynamics stem essentially from LTCs of bulk power delivery transformers. As shown in Fig. 2, the variable ratio r_i is considered to be on the primary (transmission) side and the LTC is controlling the secondary (distribution) voltage V_i. Load is considered voltage dependent. Short-term dynamics are assumed to be stable, as only long-term voltage stability issues are addressed.

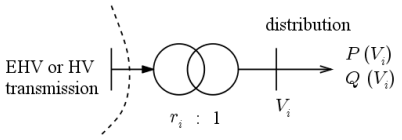

Figure 2: Transformer with LTC feeding voltage-sensitive load

Let m be the number of LTC-controlled loads. The LTC mechanisms are discrete with a voltage deadband. Thus at every period of operation T_i the i-th transformer ratio changes according to the difference equation:

$$r_i(kT_i) = r_i[(k-1)T_i] + \Delta r_i^k \tag{1}$$

with
$$\Delta r_i^k = \begin{cases} \Delta s_i & \text{if} \quad V_i > V_i^{\max} \\ 0 & \text{if} \quad V_i^{\min} \le V_i \le V_i^{\max} \\ -\Delta s_i & \text{if} \quad V_i < V_i^{\min} \end{cases} \tag{2}$$

where V_i^{min} and $V_i^{\max}$ are the lower and upper deadband limits.

The long-term stability of the system is linked to the Jacobian of secondary voltages with respect to tap ratios:

$$\mathbf{A} = \left[\partial V_i / \partial r_j \right] \qquad i, j = 1,...,m \tag{3}$$

To facilitate the analysis, at this point we assume that all LTCs have the same tap step and period of operation, i.e.

$$\Delta s_i = \Delta s \qquad T_i = T \qquad \text{for } i = 1,...,m \tag{4}$$

The general case of different tap step and time delay for each LTC can be handled by multiplying the sensitivity matrix with an appropriate diagonal matrix [14]. The application study reported in this paper includes a different time delay (period) for each LTC to show that this does not influence the validity of the results.

The vector of secondary voltage changes at each step k under the above assumptions is given approximately by the linearized expression:

$$\Delta \mathbf{V}^k = \mathbf{A}\, \Delta \mathbf{r}^k \tag{5}$$

where $\Delta\mathbf{r}$ is the vector of tap ratio changes.

Stability of this linearized discrete system is guaranteed if all voltage errors outside the deadband decrease at each step. A necessary condition to achieve this correction is that the diagonal elements a_{ii} of $\mathbf{A}$ are negative, so that each tap change performed according to (2) will decrease the error at the corresponding bus. However, this condition is not sufficient for stability because the other taps may counteract this error correction. If, however, matrix $\mathbf{A}$ is diagonally dominant with negative diagonal elements, the error correction achieved by the diagonal term cannot be counteracted whatever the direction of movement of the other taps. We thus obtain the following sufficient stability condition, originally derived in [15] (see also [16]):

$$a_{ii} + \sum_{j \ne i} \left| a_{ij} \right| < 0 \qquad i, j = 1,..,m \tag{6}$$

In the voltage stability literature, the discrete LTCs are sometimes modelled using continuous dynamics with (2) replaced by:

$$T_{ci}\, \dot{r}_i = V_i - V_i^o \tag{7}$$

where V_i^o is the voltage setpoint and T_{ci} the time constant of the i-th LTC. This continuous system representation is particularly appropriate for LTCs with inverse time delay characteristic [17]. Note that the equilibrium of (7) corresponds to the equilibrium of long-term dynamics, which implies restoration of not only secondary voltages, but also load real and reactive powers (which depend on V_i).

Linearizing (7) and making use of (3) we get for all LTCs:

$$T_c\, \Delta\dot{\mathbf{r}} = \mathbf{A}\, \Delta\mathbf{r} \tag{8}$$

which is the state space representation in the case of continuous LTC dynamics. In the sequel we will call $\mathbf{A}$ the long-term state matrix regardless of whether we refer to the continuous, or the discrete representation of LTCs. In (8) the same time constant T_c has been considered for all LTCs.

Note that (6) is also a sufficient stability condition for the continuous system (8), according to Gershgorin's theorem [18]. This theorem states that all eigenvalues lie inside disks with

centers given by the values of diagonal elements of *A* and radii equal to the sum of the absolute values of the non-diagonal elements of the corresponding row (or column). Thus, when (6) holds, there can be no zero or positive real eigenvalue.

On the other hand, it is well known that the stability limit of the continuous system (8) is met when the determinant of **A** becomes zero (saddle-node bifurcation condition). As shown in [2,8] this condition is satisfied at the so-called critical point, where the bifurcation surface in load power space is encountered during an unstable scenario.

According to the foregoing discussion, before the unstable trajectory reaches the bifurcation surface, condition (6) has to be violated for at least one LTC. Thus the violation of this condition is a precursor to hitting the maximum loadability, as it is also a precursor to instability for both continuous and discrete system representations of LTCs. Being a precursor to the exact instability condition yields interesting prediction capability to this condition for practical applications.

B. Instability Detection along a Trajectory

Let us now return to the discrete representation of LTCs (1)-(2) and assume that after a severe disturbance all voltages (at least in the area of interest) are below deadband. As a consequence, each LTC will react in every period *T* by decreasing its ratio by the amount Δs. Under these conditions, the change ΔV_i made to voltage V_i at step *k* is given by:

$$\Delta V_i^k = -\Delta s \sum_j a_{ij} = -\Delta s \,[a_{ii} + \sum_{j \neq i} a_{ij}] \qquad (9)$$

The similarity between the expression in parentheses and the sufficient stability condition (6) suggests that the change in controlled voltage could be used to monitor stability. However, before proceeding we should examine the sign of sensitivities, in order to remove the absolute value from (6).

The sign of an off-diagonal sensitivity a_{ij} can be indirectly assessed, if we assume that all loads are non-capacitive. In such cases the increase in the load consumed at bus *j* brought about by a decrease of ratio r_j will result in a decrease of transmission voltages. If all other taps remain constant, this will have the result to decrease the secondary voltages of all LTCs. Thus we have:

$$a_{ij} = \left(\frac{\Delta V_i}{\Delta r_j} \right)_{\Delta r_k = 0,\, \forall k \neq j} > 0 \qquad (10)$$

Summarizing the above discussion, when:

a) all controlled voltages are below deadband
b) conditions (10) hold
c) no other events than LTC actions occur

the sufficient stability condition (6) becomes:

$$a_{ii} + \sum_{j \neq i} a_{ij} = -\frac{\Delta V_i^k}{\Delta s} < 0 \quad \Leftrightarrow \quad \Delta V_i^k > 0 \qquad i = 1,..,m \qquad (11)$$

which suggests that, after a large disturbance, instability can be simply detected locally by monitoring an LTC-controlled voltage. Let us recall that violation of (6) detected through (11) is also a necessary condition for matrix **A** to become singular, thus instability is detected in advance, before the bifurcation surface is encountered.

Remark. For the sake of completeness, we briefly comment on the sign of the diagonal elements a_{ii}. From the previously mentioned Gershgorin's theorem, it is clear that the system is unstable if at least one diagonal element a_{ii} is positive. In other words, the diagonal elements a_{ii} must all be negative for stability. This is the case in normal loading conditions. A term a_{ii} becoming zero means that, *all ratios except the i-th one being constant*, the controlled voltage V_i goes through a maximum. Assuming that load power increases with voltage, maximizing V_i results also in maximum power consumption at the i-th bus [14]. Note that this condition is more stringent than (11).

III. Local Identifier of Voltage Emergency Situations

A. Principle of Operation

The Local Identifier of Voltage Emergency Situations (LIVES) is based upon the detection of secondary (controlled) voltages going through a maximum during the post-disturbance evolution. It could be easily incorporated into the control logic of LTCs and uses only information available in the LTC, namely secondary voltage, deadband limits and time delays between tap changes.

Two procedures will be described. The first one is a direct application of (11). It is used for comparison with the previous theoretical analysis, without considering application issues in an actual system. The second and readily applicable algorithm is based upon a moving-average filter.

In either case, LIVES logic is very simple. To initiate the detection, the LTC must be active (i.e. not limited, nor blocked), and the controlled voltage must be below its lower deadband limit. The latter is checked the first time it remains below the deadband after a tap change.

As a consequence, LIVES is reset each time the secondary voltage is restored within the deadband and becomes inactive after the LTC has exhausted its tap ratio range. The algorithms for implementing LIVES will be described for each of the two implementation procedures below.

B. Direct Voltage Comparison (theoretical procedure)

This first LIVES variant is based on the assumption of direct and accurate measurement of ΔV_i^k as defined in (5). Of course, assumption (4) cannot be guaranteed in practice, but as will be seen in the application section of this paper, different delays (as long as they are of the same order) do not hinder the emergency detection process.

In this algorithm the secondary voltage values relative to successive tap changes are compared through:

$$\Delta V_i^k = V_i(kT_i) - V_i[(k-1)T_i] \qquad (12)$$

If all LTCs have (approximately) the same time delay and no other event with the effect of lowering system voltages has occurred, a secondary voltage drop after one period of LTC operation means that the sum of the corresponding row of the long-term state matrix **A** has crossed zero and thus the sufficient stability condition is violated.

However, in a real system other events (such as generator

switching under reactive limit) may result in a voltage drop between two tap changes that is not due to the action of other LTCs. Thus an additional delay for instability detection is necessary to ascertain that voltage is dropping.

To this purpose, one can specify that ΔV_i^k must be negative for two successive values of k to detect emergency conditions. The overall delay for instability detection is in the time frame of two successive periods of LTC operation (roughly around 20 s), which is considered acceptable for emergency control against long-term voltage instability.

The algorithm executed after each tap change of the i-th LTC is summarized in the following pseudo-code:

```
IF  Vi>Vimin  THEN
    detection := off ; Vr:=0
ELSE
    IF  detection=OFF  THEN
        detection := ON ; Vr:=Vi; count:=1
    ELSE
        IF  Vi<Vr  THEN
            IF  count=1  THEN
                Vr:=Vi ; count:=2
            ELSE
                alarm issued on this LTC
            ENDIF
        ELSE
            detection := OFF
        ENDIF
    ENDIF
ENDIF
```

Clearly the algorithm ends either by issuing an alarm or by the end of detection when voltage returns in the deadband. Of course it remains possible that events cause two successive voltage drops within two periods of LTC operation. It could be argued, however, that in such a situation the system would be so weakened by these events to justify an emergency action. Nevertheless, there remains a slight risk of false alarm, if multiple events produce successive voltage depressions (violation of condition c in Section II.B), while the system is still stable.

A second problem stems from the fact that measured values of V_i are affected by system transients and measurement inaccuracies. A filtering scheme is thus needed as described in the next section.

C. Detection Based on Moving Average (practical procedure)

In this version of LIVES, the moving average of the secondary voltage in each LTC is used for emergency detection, instead of its actual measurements collected at specific time instants. The moving average at a time t_j is given by:

$$\bar{V}_i(t_j) = \frac{1}{n_i}\sum_{k=0}^{n_i-1} V_i(t_j - k\Delta t) \qquad (13)$$

where Δt is the sampling period of the measurement and n_i is the number of samples over which the moving average is calculated. Note that the average is updated at each sampling instant $t_j = j\Delta t$.

The averaging period for our application is taken equal to the corresponding LTC time delay T_i. This is done to ensure that one and only one tap change of the LTC controlling the measured voltage is included in the average (provided of course that the LTC is active). If the averaging period is taken smaller than T_i, there will be some averaging intervals that will not contain any operation of the i-th LTC, whereas if the average is taken over a time greater than T_i there will be intervals with two tap changes and others with only one. Thus, the averaging will not have the smoothing effect intended and will not approximate correctly the general trend of V_i.

Note that the averaging period is thus different for each measured voltage. The number of samples for each average is given by $n_i = T_i / \Delta t$.

The averaging helps to filter out fast transients (caused for instance by electromechanical oscillations) and measurement noise. It is also used as an indirect record of the period just prior to a tap change. Thus, using the moving average the emergency detection process implicitly includes the information of voltage evolution of the period before LTC tap changing. As a result, just one period of LTC operation is enough to detect an emergency.

In the ideal case where only LTCs are acting and all time delays are equal, the moving average immediately after a tap change occurring at $t_k = kT_i$ will vary by the following amount, which is found by directly substituting the moving average from (13) and making the obvious cancellation of terms except the first and last ones:

$$\bar{V}_i(kT_i) - \bar{V}_i(kT_i - \Delta t) = \frac{1}{n_i}\left[V_i(kT_i) - V_i(kT_i - T_i)\right] = \frac{1}{n_i}\Delta V_i^k \qquad (14)$$

with ΔV_i^k as defined in (12). Thus the sufficient stability condition (11) is equivalent to an increasing moving average after a tap change:

$$\bar{V}_i(kT_i) - \bar{V}_i(kT_i - \Delta t) > 0 \qquad (15)$$

Furthermore, the moving average value at the time t_k of the k-th tap change is taken as a reference for monitoring the subsequent evolution of the moving average over the time interval $[t_k \quad t_k + T_i + \varepsilon]$. This reference is denoted as $V_{ri}(t)$ with:

$$V_{ri}(t_j) = \bar{V}_i(t_k) \qquad t_j \in \left[t_k \quad t_k + T_i + \varepsilon\right] \qquad (16)$$

The term ε is introduced for added security purposes, i.e. to benefit from a longer observation period, allowing time for voltage recovery in a marginally stable case. The added delay (typically a couple of seconds) is not critical for long-term instability detection.

More precisely, the detector timer starts to count at $t=t_k$ and:

- if at a time $t_j > t_k$ the average voltage $\bar{V}_i(t_j)$ increases above $V_{ri}(t_j)$, the counter is immediately reset; the process will repeat itself after the next tap change;
- if the voltage average $\bar{V}_i(t_j)$ remains below $V_{ri}(t_j)$ for a time equal to the period T_i of LTC operation, plus an optional added delay ε, an emergency signal is issued.

As shown above, this detection process is similar in principle to that of comparing the successive post-taping voltages,

but without the dangers associated with comparing two isolated measurements.

IV. Simulation Results

A. Test System

The so-called Nordic32 test system detailed in [19] has been used to check the proposed method. The system includes 52 EHV and HV buses, 19 generators and one synchronous condenser, as shown in Fig. 3.

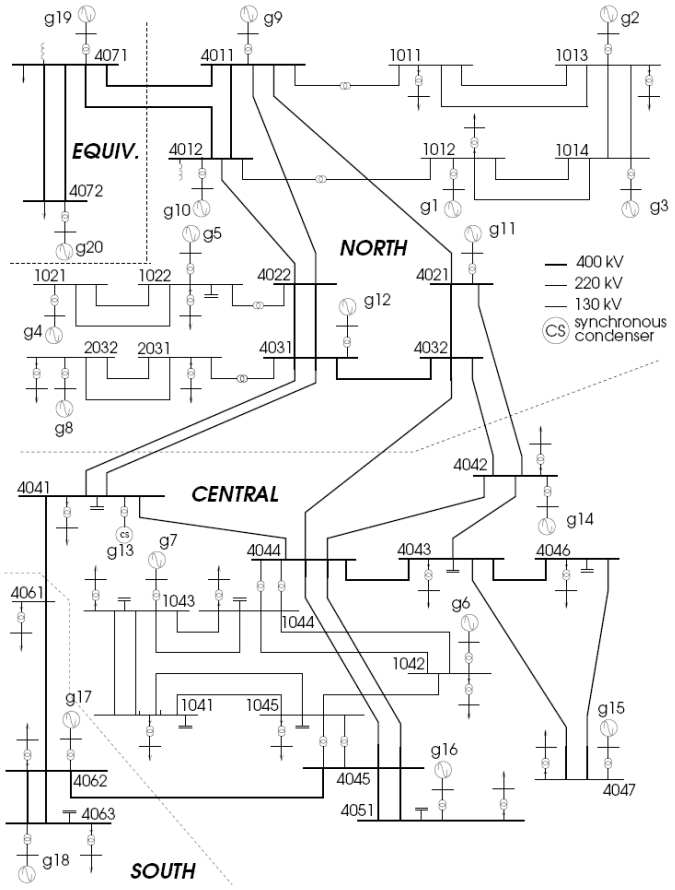

Figure 3: Nordic32 test system

Voltage magnitude signals have been obtained from detailed time simulations using the SIMULINK library described in [20]. The short-term dynamics includes 5th- and 6th-order models of synchronous machines, together with AVR, prime mover and speed governor models. The long-term dynamics are driven by the 22 LTCs on transformers feeding respective MV distribution buses, as well as by OELs on the generators. The latter are of the takeover type [2], and act after various overexcitation periods. MV bus numbers are not shown in Fig. 3 to preserve clarity. These buses are named with the "MV-" prefix in the text. For instance "MV-1041" is the MV bus behind the distribution transformer connected to HV bus 1041. An exponential model is used to represent the load dependency on voltage, at MV buses, with exponent 1 (constant current) for active power and 2 (constant admittance) for reactive power. Since the tap changes are used for instability detection, care was taken in the simulation that the LTCs are not synchronized, so as to have a more realistic situation. This was achieved by using different values for the first and subsequent tap-change delays of each LTC. The LTC parameters used in the simulation are summarized in Table III of the Appendix.

B. Case Studies

In the above system we first consider a stressed operating condition (Case 1), for which the single trip of line 4032-4044 at time t= 1s initiates a voltage collapse in the Central area of the system (see Fig. 3), as seen in Fig. 4, which shows voltages at HV buses in the affected area. Voltages oscillate under the effect of rotor swings and eventually plunge due to a loss of synchronism of the field-current-limited generator g6.

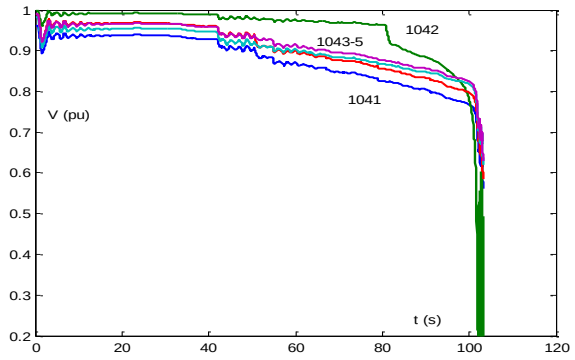

Figure 4: Case 1: evolution of voltages at HV buses

Table I shows the sequence of events. The first column gives simulation times, the second column the activation of OELs, and the third one the tapping of LTCs. Successive tap changes of the same LTC are marked by letters a, b, etc. (the other information in this table will be referred to in the sequel). As seen in this table, 30 s after the disturbance all LTCs in the affected Central area of the system start operating. Most controlled voltages in the area remain below their deadbands.

Further tests have been performed to check the ability of LIVES to provide a warning in less pronounced instability cases, as well as to avoid false alarms in marginally stable voltage situations. Two other cases are shown in this paper, which were obtained by modifying the initial loading condition, so that the examined contingency (which is the most severe) will result in marginal stability or instability.

In Case 2, the load in the Central area was decreased by 240 MW / 80 Mvar. The system is still unstable, but the instability takes a long time to manifest itself as shown in Fig. 5.

In Case 3, a further pre-disturbance load decrease of 30 MW / 10 Mvar was considered. The response to the same disturbance is shown in Fig. 6. Even though the system takes a long time to settle down, the LTCs are able to return their corresponding controlled voltages within the deadbands, so that a stable steady state is reached.

The summary of events during simulation of cases 2 and 3 is given in Table II. The difference between these two cases is the successive limitations of generators g15, g16, and g12, which do not take place in Case 3.

C. Case 1: detection by direct voltage comparison

We consider in this section the criterion of two direct post-tap-change voltage comparisons.

TABLE I: SEQUENCE OF EVENTS IN CASE 1

time (s)	OEL	LTC connected to bus	detection by	
			direct V change	moving average
31.0		1041 a		
33.0		1043 a		
34.0		1044 a		
35.0		1045 a		
36.0		4041 a		
37.0		4042 a 4051		
38.0		4043 a		
39.0		4046 a		
42.0	g14	1043 b (+)		
43.0		1041 b (-)		
43.7	g15			
44.0		1044 b (-)		
45.0		4041 b (+)		
46.0		1045 b (-) 4047 a		
46.2	g12			
47.0		4042 b (-)		
49.0		4043 b (-)		
50.5	g7			
51.0		1043 c (-) 4046 b (-)		
54.0		1044 c (+) 4041 c (+) 4047 b (-)		1044 4047
54.8	g16			
55.0		1041 c (-)	1041	1041
57.0		1045 c (-) 4042 c (-)	1045 4042	1045 4042
60.0		1043 d (-) 4043 c (-)	1043 4043	1043 4043
62.0		4047 c (-)	4047	
63.0		4041 d (+) 4046 c (-)	4046	4046
64.0		1044 d (-)		
68.0		1042 a		
74.0		1044 e (-)	1044	
76.0		1042 b (+)		
76.6		4051 a		
80.7	g6			
84.0		1042 c (-) 4061 a		
85.6		4051 b (-)		4051
92.0		1042 d (-)	1042	1042
94.0		4061 b (+)		
94.6		4051 c (-)	4051	
102.0	loss of synchronism (g6) - collapse			

In Table I, a positive sign (+) after the tapping indication means that ΔV_i^k is positive, a negative sign (-) that it is negative. The first bus where emergency is detected is 1041 at t=55s, as shown in the fourth column of Table I. In the next few seconds, emergency detection signals are also issued at other six buses (1045, 4042, 1043, 4047, 4046, and 1044). The voltages at buses MV-1042 and MV-4051 re-enter their deadbands for a while, thereby resetting the instability detection process, but subsequently leave them again, and the emergency is detected at these two buses shortly before the collapse (at t= 92 s and 94.6 s respectively).

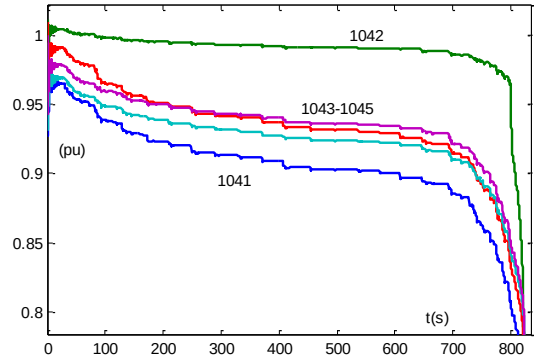

Figure 5: Case 2: evolution of voltage at HV buses

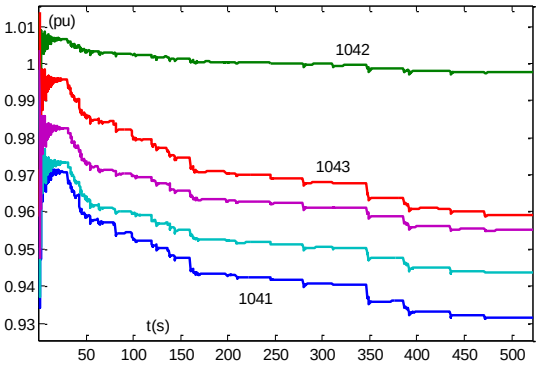

Figure 6: Case 3: evolution of voltage at HV buses

TABLE II. SEQUENCE OF EVENTS IN CASES 2 AND 3

t (s)	Case 2		Case 3	
	OEL	LIVES	OEL	LIVES
85.7	g7			
92.0	g14			
99.1			g7	
143.5			g14	
475.0			steady state (stable)	
496.1	g15			
663.6	g16			
693.1	g12			
753.3		1041		
787.4		1045		
788.4		4046		
788.8		4051		
796.5		4043		
798.1		1043		
800.5	g6			
804.2		4047		
805.4		1044		
811.3		4042		
814.5		1042		
825.3	collapse			

All LTCs in the South and North areas are able to keep

their voltages within the deadband, so the emergency detection process in these areas never starts, or is immediately reset after the first successful tap change.

In Fig. 7 the voltage of bus MV-1041 is shown near the time of instability detection. The stars indicate the voltage values used to compute ΔV^k. It should be noted in this figure that the emergency detection is brought about by the field current limitation of g14 and g7 that take place in two successive periods of tap operation. This should not be considered a misoperation, as the cascaded limitation of generating units is also a major factor precipitating voltage collapse.

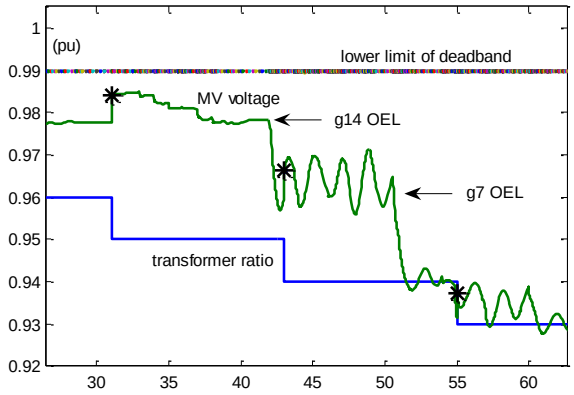

Figure 7: Voltage at bus MV-1041 and ratio of controlling transformer

D. Case 1: detection based on Moving Average

The tests reported in the remaining of the paper have been performed with measurement noise added to each voltage obtained from time simulation. The random noise is uniformly distributed in the [-0.001 +0.001] pu interval (in the sequel, we refer to this simulated voltage measurement as "voltage measurement", for the sake of simplicity).

The procedure of Section III.C has been applied, with a sampling period Δt =50 ms used to simulate the measurement system and compute each moving average. The latter is computed over a time window equal to the delay between two successive tap changes. Let us recall that the averaging is performed continuously, but the detection process starts after the LTC has acted for the first time. The emergency detection signals issued at each bus are shown in the last column of Table I. The optional additional time delay ε is not considered in this table.

The noisy measurement signal, its moving average, the reference voltage of (16) and the transformer ratio are shown in Fig. 8 for bus MV-1041. The detection process starts after the first tap at time t =31s. As seen in Fig. 8, the moving average is increasing immediately after this point, thus the counter for emergency detection is reset until the next tap change, which occurs at t =43s. After this point, the average drops continuously for the full LTC time delay of 12s, and thus the emergency detection signal is issued at t =55s. In this particular case, this is identical to the detection time based on direct post-tap-change voltage comparison. Note that the overall decline of the average was present even without the g7 limitation occurring at t =50.5 s.

As seen in Table I, at all buses the emergency detection was performed either at the same time, or faster, when using the moving average method. The improved anticipation capability is noticeable at buses MV-1044, MV-4047 and MV-4051. This is because the moving average method requires a time delay of only one LTC period, since it implicitly compares also with the previous values stored in the moving average, as discussed in Section III.C. For instance, in the case of bus MV-1044, shown in Fig. 9, the overexcitation limitation of generator g14 (at t = 42s) takes place just before the second tap change (at t =44s) and causes the post-tap-change voltage to be low. As a result, the voltage is higher after the third tap change (at t = 54s) than after the second one, and the condition of two successive post-tap-change voltage reductions is not met before t =74s (see Table I). The moving average, on the other hand, shows a clear decline after the tap change at t=44 s; therefore, emergency is detected at t =54s.

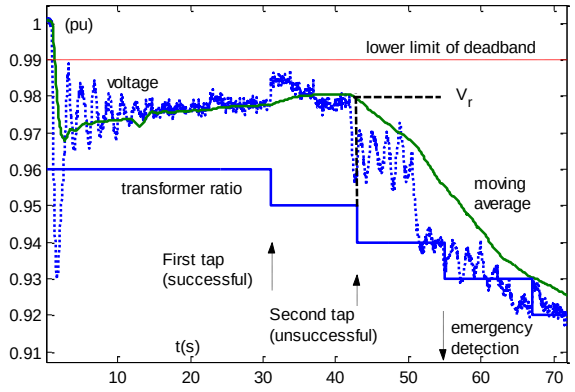

Figure 8: Voltage measurement, moving average and ratio at bus MV-1041

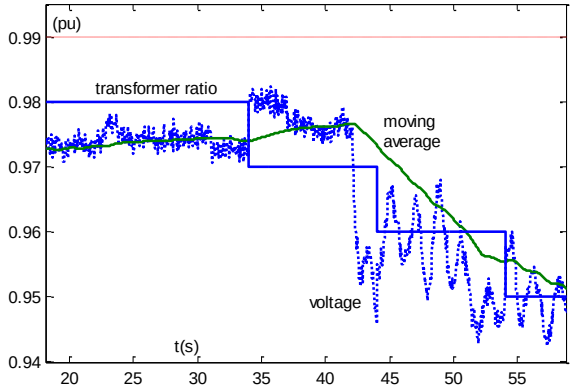

Figure 9: Voltage measurement, moving average and ratio at bus MV-1044

Another interesting case is that of bus MV-4041, shown in Fig. 10. This is a boundary bus, connecting the affected Central area to the South and North parts of the system, which are little affected by the voltage instability. This bus is next to a synchronous condenser that keeps controlling voltage throughout the simulation. In fact the voltage control of this bus is stable, since as seen in Table I the LTC is able to bring the secondary voltage inside its deadband after four tap changes. Observing Fig. 10 it is seen that the moving average voltage starts decreasing after t =42s due to the limitation of a nearby

generator, but the trend reverses some time after the second tap change. When the moving average signal crosses its reference V_{ri} at t =52s, the detection process is reset.

This example shows that the emergency detection based on the moving average is able to discriminate successfully between stable and unstable LTCs and thus avoid a false alarm.

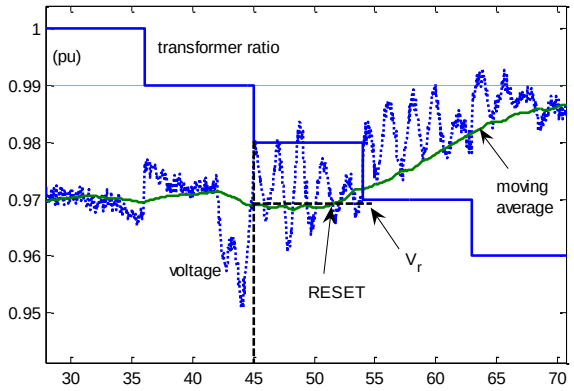

Figure 10: Voltage measurement, moving average and ratio at bus MV-4041

Another marginal case is that of bus 4042 (see Fig. 11). This bus is on the border between North and Central areas, but as generator g14 connected to this bus gets limited at t =42s, it participates in the instability. As seen in Fig. 11, the average voltage never recovers above the value V_{ri} (reference after the second tap change) and therefore an alarm is issued at t =57s. Even though the average voltage settles for a few seconds at 0.94 pu, it eventually plunges down as the system collapses (see Fig. 4). In any case, while the LTC is within its control range, the controlled voltage should recover and not stay at values below deadband.

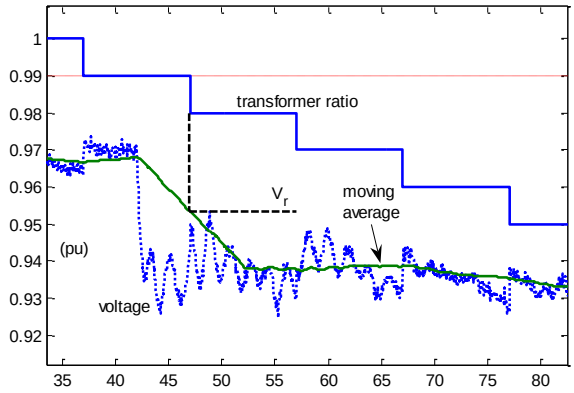

Figure 11: Voltage measurement, moving average and ratio at bus MV-4042

The above examples demonstrate the ability of the proposed procedure to detect promptly and securely imminent voltage instability and also to identify accurately the load buses where instability is evolving.

E. Analysis of Case 2 (marginally unstable)

As shown in Table II, in Case 2 LIVES started detecting emergency conditions roughly one minute after the series of generator limitations and more than one minute before the final collapse.

One of the difficulties encountered in Case 2 was that some taps reached the lower limit (88%) of their control range. This, however, did not prevent the emergency detection process to produce a clear emergency alarm. For instance, at bus MV-1041 the LTC limit was reached with the tap movement made at t =741.3 s. After this the moving average signal remains below V_r, as shown in Fig. 12, and thus an emergency detection signal is issued after the time interval T_i, at t =753.3 s.

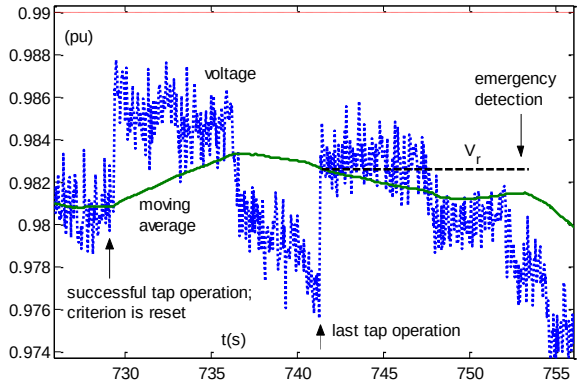

Figure 12: Voltage measurement and moving average at bus MV-1041

The most difficult detection was at bus MV-1044. As seen in Fig. 13, the tap change at t =795.4 s (close to the time of collapse) only marginally failed to restore the moving average of measured voltage and thus an emergency detection alarm was issued 10 s later, i.e. at t =805.4 s.

The detection occurred even later at bus 1042 (at t =814.5s, roughly 10s before the collapse), but detection was slow at this bus even in the severe instability case, due to the fact that its voltage is supported by generator g6 which is the last one to switch under field current limit and the first one to lose synchronism after the limit is enforced.

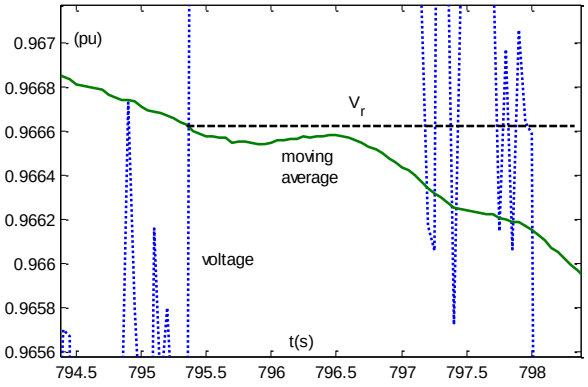

Figure 13: Voltage measurement and moving average at bus MV-1044

A last interesting case is shown in Fig. 14 for bus MV-4046, where the detection counter was reset three times before finally giving the emergency detection signal at t =788.4 s.

As seen, even in this marginal case the procedure was able to detect emergency conditions in time for emergency control, at all ten affected buses. Again, no false alarm was given at the

boundary stable bus MV-4041, or at any other bus.

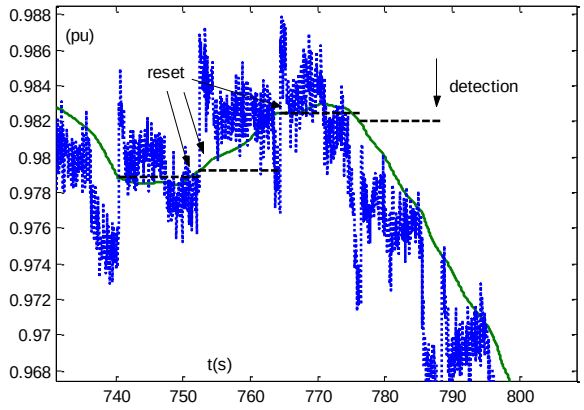

Figure 14: Voltage measurement and moving average at bus MV-4046

F. Analysis of Case 3 (marginally stable)

In the marginally stable situation of Case 3, the LTCs are able to bring back their corresponding voltages within the deadband, and hence the emergency detection process is reset without issuing any alarm. This is shown in Fig. 15, where the simulated secondary voltage and its moving average are plotted for the LTC of bus 1041, which has the lowest primary (HV) voltage for the contingency of concern. As seen in the figure, the LTC acts five times, and each action restores the MV voltage within the deadband. Thus the emergency detection counter is never even initiated.

This case illustrates that LIVES is unlikely to yield a false alarm even in a marginally stable situation. This is a promising result concerning the selectivity of the proposed indicator.

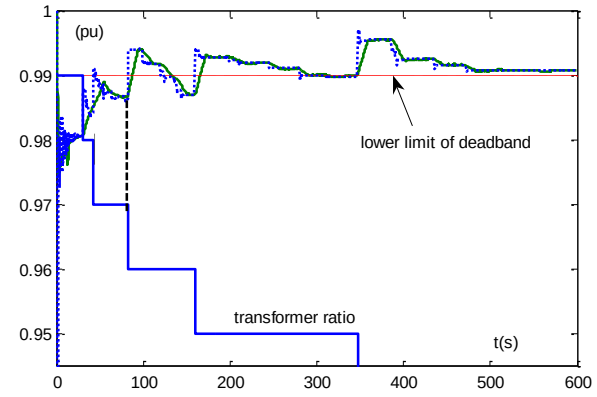

Figure 15: Voltage measurement, moving average, and ratio at bus MV-1041

V. Discussion and Conclusion

This paper presented a simple and effective design of a local voltage emergency identifier based on monitoring the controlled distribution voltage of LTC transformers.

Detailed simulation results in a small but realistic power system have shown that the proposed detection process was able to signal out a voltage emergency situation for all affected buses in two unstable cases, without yielding a false alarm for unaffected buses. Also, no false alarm was issued in a marginally stable case.

The above results encourage the use of the LIVES method to provide a triggering signal for load-shedding system protection schemes. Load could be shed either locally from the bus where an emergency alarm is issued, or in a coordinated manner, e.g. in conjunction with an Under Voltage Load Shedding system (UVLS). One point in favor of shedding load from a bus where LIVES has detected an emergency is that at this bus load cannot be restored anyway, as the distribution voltage remains below deadband, whereas a load shedding action will immediately restore voltage and thus the remaining load demand.

In fact, a most promising application of LIVES could be its use as a complement to existing or under design UVLS schemes. For instance, LIVES can export, together with the emergency detection signal, the transmission side voltage and the exact time of detection using some synchronized time measurement. This information can then be taken into account for the automated on-line tuning of the UVLS scheme.

Concerning the timing of alarm issuing, for the system considered (e.g. Case 2) the undervoltage condition would most probably be detected at bus 1041 sooner than the LIVES alarm. However, as all other HV buses remain above 0.9 pu for a long time, it would be quite difficult to take a load shedding decision without the positive emergency detection provided by LIVES. Again the complementarity with UVLS is evident.

Further research is definitely necessary to integrate LIVES in an actual SPS. However, the initial results reported in this paper are certainly encouraging.

Appendix. LTC Data of Test System

All transformers feeding loads are equipped with LTCs and their ratios may vary between 0.88 and 1.20 by steps of 0.01 pu/pu, thus yielding 33 tap positions. All LTC voltage setpoints are set to 1.00 pu, with a deadband V_i^{max}-V_i^{min} of 0.02 pu. Table III provides the individual tapping delays and initial ratios (in Case 1). Let us recall that the latter are decreased to increase distribution voltages, according to (2).

Table III. LTC Data of Nordic32 System

bus	delay on first tap change (s)	delay on next tap changes (s)	initial ratio
1011	30	8	1.02
1012	30	9	1.03
1013	30	10	1.05
1022	30	11	1.06
1041	30	12	0.96
1042	31	8	1.00
1043	32	9	0.99
1044	33	10	0.98
1045	34	11	0.99
2031	30	12	1.05
2032	30	8	1.10
4041	35	9	1.00
4042	36	10	1.00
4043	37	11	0.99
4046	38	12	0.99
4047	39	8	1.02

4051	30	9	1.02
4061	30	10	0.98
4062	30	11	1.00
4063	30	12	1.00
4071	30	9	1.01
4072	30	11	1.01

REFERENCES

[1] C. Taylor, *Power system voltage stability*, EPRI Power System Engineering Series, Mc Graw-Hill, 1994

[2] T. Van Cutsem, C. Vournas, *Voltage Stability of Electric Power Systems,* Kluwer Academic Publishers, 1998

[3] C. Taylor, "Concepts of undervoltage load shedding for voltage stability", IEEE Trans. on Power Delivery, Vol. 7, pp. 480-488, 1992

[4] D. Lefebvre, S. Bernard, T. Van Cutsem, "Undervoltage load shedding scheme for the Hydro-Québec system", Proc. IEEE PES General Meeting, Denver, 2004

[5] S. Imai, "Undervoltage load shedding improving security as reasonable measure for extreme contingencies", Prof. IEEE PES General Meeting, San Francisco, 2005

[6] C. Rehtanz (convenor), "Wide area monitoring and control for transmission capability enhancement", Final report of CIGRE Working Group C4.601, CIGRE technical brochure, Dec. 2006

[7] B. Gao, G.K. Morison, P. Kundur, "Voltage stability evaluation using modal analysis", IEEE Trans. on Power Systems, Vol. 7, 1992, pp. 1529-1542

[8] F. Capitanescu, T. Van Cutsem, "Unified sensitivity analysis of unstable or low voltages caused by load increases or contingencies", IEEE Trans. on Power Systems, Vol. 20, 2005, pp. 321-329

[9] M. Begovic, K. Vu, D. Novosel, M. Saha, "Use of local measurements to estimate voltage stability margins", IEEE Trans. on Power Systems, Vol. 14, 1999, pp. 1029-1035

[10] A. Holen, L. Warland, "Estimation of distance to voltage collapse: testing an algorithm based on local measurements", Proc. 14th Power System Computation Conference, Sevilla, 2002, paper 38-3

[11] B. Milosevic, M. Begovic, "Voltage-stability protection and control using a wide-area network of phasor measurements", IEEE Trans. on Power Systems, Vol. 18, 2003, pp. 121-127.

[12] H. Ohtsuki, A. Yokoyama, Y. Sekine, "Reverse Action of On-Load Tap Changer in Association with Voltage Collapse", IEEE Trans. on Power Systems, vol. 6, pp. 300-306, Feb. 1991.

[13] "Application Manual for Power Transformer Protection and Control Terminal", p. 149, ABB Document: 1MRK504037-UEN, available from http://www.abb.com/Product/seitp332/c1256ccb004e670dc125697700340390.aspx

[14] C. D. Vournas and N. G. Sakellaridis, "Region of Attraction in a Power System with Discrete LTCs", IEEE Trans. on Circuits & Systems I, vol. 53, pp. 1610--1618, July 2006.

[15] J. Medanic, M. Ilic-Spong, and J. Christensen, "Discrete Models of slow voltage dynamics for under load tap-changing transformer coordination", IEEE Trans. on Power Systems, vol. 2, pp. 873-882, Nov. 1987.

[16] N. Yorino, M. Danyoshi, M. Kitagawa, "Interaction Among Multiple Controls in Tap Change Under Load Transformers", IEEE Trans. on Power Systems, Vol. 12, pp. 430 – 436, Feb. 1997.

[17] P. W. Sauer, M. A. Pai, "A Comparison of Discrete vs Continuous Dynamic Models of Tap -Changing - Under - Load Transformers", Bulk Power System Voltage Phenomena – III, Davos, pp. 643-650, Aug. 1994.

[18] A. Jennings, Matrix computation for engineers and scientists, John Wiley & Sons, 1977.

[19] CIGRE TF 38.02.08 (M. Stubbe, convenor), ``Long-term dynamics - Phase II", Final report, January 1995.

[20] C. D. Vournas, E. G. Potamianakis, C. Moors, T. Van Cutsem, "An educational simulation tool for power system control and stability", IEEE Trans. on Power Systems, vol. 19, pp. 48-55, Feb. 2004.

BIOGRAPHIES

Costas D. Vournas (S'77 - M'87 - SM'95 - F'05) received the Diploma of Electrical and Mechanical Engineering from the National Technical University of Athens (NTUA) in 1975, the MSc in Electrical Engineering from the University of Saskatchewan in 1976, and the Doctor of Engineering again from NTUA in 1986. He is currently Professor in the Electrical Energy Systems Laboratory of the School of Electrical and Computer Engineering of NTUA. His research interests are in the area of power system dynamics, stability and control with emphasis on voltage stability analysis.

Thierry Van Cutsem (M'94 - SM'03 - F'05) graduated in Electrical-Mechanical Engineering from the University of Liège, where he obtained the Ph.D. degree and is now adjunct professor. Since 1980 he has been with the Fund for Scientific Research (FNRS), of which he is now a Research Director. His research interests are in power system dynamics, stability, security, optimization and real-time control, in particular voltage stability and security.